Development of an Infrared Absorption Spectroscope Based on Linear Variable Filters

Felipe G. Nogueira, Daniel Felps, and Ricardo Gutierrez-Osuna, *Member, IEEE*

***Abstract*—The objective of this research is to develop a low-cost infrared absorption spectroscope based on linear variable filter technology for the automated detection of concentrated gases and vapors, and the semiautomated detection of liquids. This instrument represents an alternative to electronic-nose devices based on cross-selective gas sensor arrays. Instead, the proposed instrument uses the concept of computational "pseudosensors," whereby spectral lines in an analytical instrument are clustered into groups and used as independent variables. We characterize the system on a database of chemical mixtures, and evaluate it on two real-world applications in the foodstuffs domain: oil adulteration and trans-fatty acid detection. Our results show that the proposed system is a viable low-resolution, low-cost analytical technique for niche applications.**

***Index Terms*—Electronic nose technology, infrared spectroscopy, linear variable filters, pattern classification.**

I. Introduction

ARRAYS of cross-selective chemical sensors, commonly referred to as electronic noses, have been developed during the past two decades as a low-cost alternative for the analysis of volatile compounds [1]. The e-nose approach is very effective when one wishes to obtain a holistic response to the sample. However, since the detection principle in these instruments is combinatorial (i.e., many volatiles are detected by a single sensor, and *vice versa*), it becomes challenging to determine the extent to which one specific component in a complex sample is responsible for the response of the array. For instance, Pinheiro *et al.*[2] showed that the response of an e-nose to the headspace of wine during the fermentation process is due to the alcohol content of the wine rather than its aroma. Thus, this form of proxy measurements (i.e., the target analyte is correlated with an easily measurable variable) can be misleading. Further, e-noses are limited to the analysis of volatile species, which may have a different composition than the liquid (or solid) sample that one is interested in analyzing.

In analogy with the e-nose paradigm, an array of "pseudosensors" may be obtained by selectively clustering the response of an analytical instrument, i.e., retention time in a gas chromatograph, absorption wavelengths in a Fourier transform infrared spectrometer (FTIR), or mass/charge ratios in a mass spectrometer [3]. To date, the use of this approach has been limited to laboratory settings due to the cost and size of the instruments. Advances in micro and nanofabrication technology are, however, likely to overcome these issues [4][5]. Along these lines, Rubio *et al.* [6] have shown that an infrared (IR) detector can be coupled with a Fabry–Perot tunable filter to produce a miniaturized IR spectrometer. In a related paper, the authors propose to use an optical filter array atop a thermopile array [7]. Among the advantages of this approach over traditional e-nose instruments are interpretability (i.e., the ability to correlate spectral features with molecular structure) and contact-free sensing, which helps prevent sensor drift and poisoning. On the downside, the sensitivity of IR-based devices can be significantly lower than that of e-noses based on solid-state sensors.

In contrast with the abovementioned efforts on IR sensing [6], [7], this work employs a linear variable filter (LVF), which serves as a bank of optical filters, coupled with a pyroelectric detector array. The advantage of this approach is that the array response can be easily interpreted as a low-resolution IR absorption spectrum. When compared with analytical techniques such as FTIR spectroscopy, LVF-based spectroscopy has lower signal-to-noise ratio (SNR) and reduced resolving power, which makes the characterization of similar compounds more involved. However, these issues can be overcome by employing robust signal processing techniques as shown by the results in this paper.

This paper is organized as follows. Section II provides a brief background review on infrared absorption spectroscopy. Section III presents a description of the instrument and its different building blocks. The instrument is then validated on three different experiments. In the first experiment, described in Section IV, the system is used to estimate the concentration of an analyte in the presence of other IR absorbing species in the gas phase. In contrast, the second and third experiments are performed in the liquid phase, as described in Section V. In the second experiment, the system is used to discriminate different edible oils in the liquid phase. Finally, in the third experiment, the system is used to detect different levels of trans-fatty acids (TFAs) in margarines and spreads. These two application scenarios are chosen to illustrate the potential of the technology for rapid, low-cost analysis in the foodstuffs industry.

II. Background Review

IR absorption spectroscopy strides to determine the differences in energy caused by the absorption of IR radiation when reflected from or transmitted through a medium. In order for IR absorption to occur, energy must cause a change in a molecule's electric dipole moment, exciting a molecule to higher degrees of

Manuscript received September 14, 2006; revised November 18, 2006; accepted February 22, 2007. This work was supported in part by the National Science Foundation under CAREER Grant 9984426/0229598. The associate editor coordinating the review of this paper and approving it for publication was Prof. William Tang.

The authors are with the Department of Computer Science, Texas A&M University, College Station, TX 77840 USA (e-mail: fgn@tamu.edu; dlfelps@tamu.edu; rgutier@cs.tamu.edu).

Color versions of one or more of the figures in this paper are available online at http://ieeexplore.ieee.org.

Digital Object Identifier 10.1109/JSEN.2007.901002

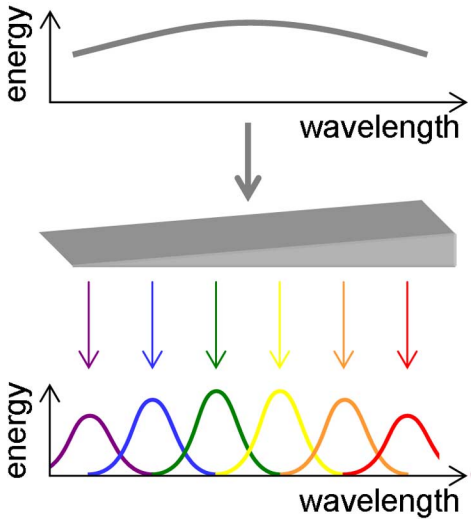

Fig. 1. Illustration of an LVF. The device operates as a Fabry–Perot interferometer, selectively allowing wavelengths to pass in proportion to the thickness of the wedge.

vibration and rotation [8]. Because of its particular bonds and molecular structures, each chemical species produces a unique IR absorption spectrum, which can be used for analytical purposes. The IR spectrum ranges from 0.75 μm to 1 mm, and is conventionally divided into far-, mid- and near-IR regions. The far-IR region is commonly used for molecular rotational spectroscopy of molecules containing heavy atoms. The mid-IR region is typically used for molecular rotation-vibration spectroscopy at harmonic frequencies, whereas the near-IR region is used for the overtones and combination of certain bands in the mid-IR region [8]. The mid-IR region is further subdivided into functional and fingerprint regions. The functional region is considered to show absorption due to molecular functional groups, whereas the fingerprint region is considered to show absorption due to intrinsic skeletal vibrations, which are unique to each molecule. Thus, the functional region is useful for characterization, since absorption bands at this region indicate the presence of certain molecular bonds and structures, whereas the fingerprint region is useful for classification.

To a first order of approximation, IR absorption follows the Beer–Lambert (B-L) Law, which states that the amount of absorption suffered by an IR radiation beam when transmitted through a sample is proportional to the path traveled and the sample concentration

$$A = \varepsilon c l \tag{1}$$

where A is absorption, ε is the absorptivity coefficient, and l is the path length. Under nonideal operating conditions (e.g., scattering, refraction), however, the B-L Law requires modifications to account for additional properties of the interaction between light and matter. A comprehensive discussion on the B-L Law is provided elsewhere [9].

III. System Description

At the core of our system is an IR detector that combines an LVF and an array of 64 pyroelectric detectors (IR Microsystems; Lausanne, Switzerland). Illustrated in Fig. 1, the LVF is

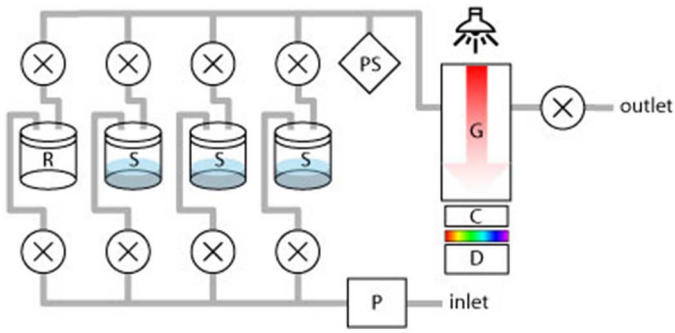

Fig. 2. High-level schematic diagram; P: pump, R: reference gas, S: samples, PS: pressure sensor, G: gas cell, C: mechanical chopper, and D: detector. The LVF is placed between the chopper and the detector.

a wedge-shaped interference filter, which provides a bank of transmission wavelengths from the thinnest end (short wavelengths) to the thickest (long wavelengths.) In our case, the LVF covers the range 5.27–10.5 μm (i.e., 1898–955 cm^{-1}), which spans a large portion of the mid-IR fingerprint and functional regions, with an intrinsic resolution of 1.5% of the transmitted wavelength. The LVF sits atop a 64-pixel pyroelectric detector array, which has a surface area of 14.7 $\times$ 3.5 mm^2 and pixel pitch of 0.2 mm (interlaced). Each pixel in the array extends an area of 0.12 $\times$ 1 mm^2.

In addition to the detector, the instrument is composed of an IR source, mechanical chopper, gas chamber, air pump, valves, and a pressure sensor. Fig. 2 shows a high-level block diagram of the system. The system uses a 10 cm gas cell (Buck Scientific; East Norwalk, CT) as the gas chamber. Two zinc selenide (ZnSe) windows (25 mm diameter, 4 mm thickness) are used for the ends of the gas cell (Cradley Crystals Corporation; Nizhni Novgorod, Russia.) Though significantly more expensive than other materials (e.g., NaCl, KBr), ZnSe can withstand exposure to most nonacidic solvents, and has low absorption in the mid-IR region, making it ideal for our purposes. The windows have an anti-reflective coating to minimize intensity losses.

The delivery system uses an oil-less diaphragm pump (GAST; Benton Harbor, MI) capable of 15-psig maximum pressure. We employ the pump in pressure mode in order to pressurize the gas chamber, which increases the SNR for low-concentrated gases . The gas circuit begins at the air inlet of the diaphragm pump, and continues through a four-valve manifold, as illustrated in Fig. 2. The valve system defines the flow path, allowing only a particular or a combination of samples to be in the gas circuit. The headspace of the sample container(s) is pushed to a gas cell and pressurized to 12 psi, as measured with a miniature pressure sensor (Honeywell; Freeport, IL). The radiation emitted by the IR source is transmitted and absorbed at certain wavelengths by the gas sample, modulated by the chopper, selectively filtered by the LVF, and finally measured at the detector array. The user controls the system via a graphical user interface and scripting tool on a personal computer. The cost for the system, including all off-the-shelf and custom parts but excluding the personal computer, totaled under US$6000. This price compares favorably with commercial FTIR systems, whose prices are in the order of tens of thousands of dollars.

TABLE I
MIXTURE COMPOSITION (% V/V)

No.	*Acetone*	*Witch hazel*	*Water*	*Alcohol*
1	6	5	90	0
2	2	18	80	0
3	4	0	50	46
4	1	0	70	29
5	8	0	80	12
6	8	0	90	2
7	2	0	80	18
8	6	0	34	60
9	10	30	60	0
10	0	40	30	30
11	0	40	30	30
12	0	60	40	0
13	10	10	70	10

We have evaluated the system on a number of performance metrics including repeatability, linearity, sensitivity and drift; uncovering the system's detection limits and resolving power. The system's combined expanded uncertainty was estimated to be 11.12%. The output of the system changes linearly with the concentration of the sample, provided that the system is used within the B-L useful range. A steady-state response is reached within one sampling period (1 s); thus 100% of the full scale can be read in 1 s, which is in pair with the scan time required by most MIR spectrometers on the market today. Since the samples are never in contact with the detector, the system does not suffer from drift/poisoning problems. Resolution is dependent on the size of the detector array (in pixels) and the quality of light collimation. The latter depends on the parabolic mirror used and the emitter-detector distance; when the emitter is moved away from the detector, source intensity decreases but resolution increases. Nonetheless, resolution is bound by the resolving power of the system, given by the detector array size (i.e., $R = 64$). The detection limits for IR absorption instruments cannot be generalized for all chemical species because of their different absorption spectra. In Sections IV and V, we provide experiments which estimate the detection and discrimination capability of the system for specific applications in the foodstuff industry.

Lock-in chemical excitation is used to increase the SNR of the instrument. Lock-in amplifiers are commonly used to extract signals with a known carrier from a noisy environment. The signal to be measured is modulated with a carrier frequency, then amplified with a bandpass filter tuned to the carrier frequency [10]. We extend this basic idea as a sampling technique by intermittently delivering chemical vapors and a reference gas to the gas cell, and measuring the AC amplitude of the response at each pixel in the array. By allowing the frequency of chemical modulation to be lower than that of the noise, the latter can then be averaged out.

IV. EXPERIMENTAL: MULTICOMPONENT ANALYSIS

The system is first validated in a mixture processing problem. For this purpose, various concentrations of an analyte (acetone) were prepared in a matrix of interfering absorbing species (water, isopropyl alcohol, and witch hazel), according to the concentrations in Table I. These analytes were chosen to obtain a mixture of simple (e.g., acetone) and complex (e.g., witch hazel) absorbing species in highly concentrated gas form.

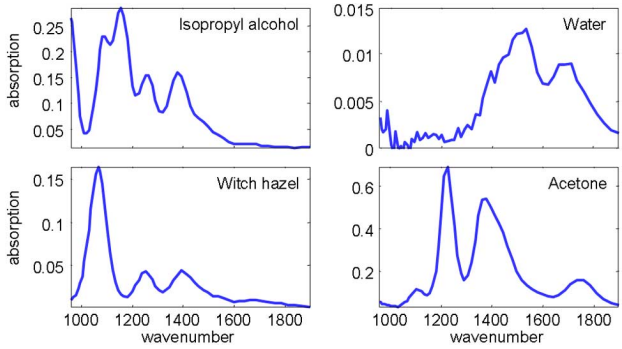

Fig. 3. IR absorption spectra of the four mixture components.

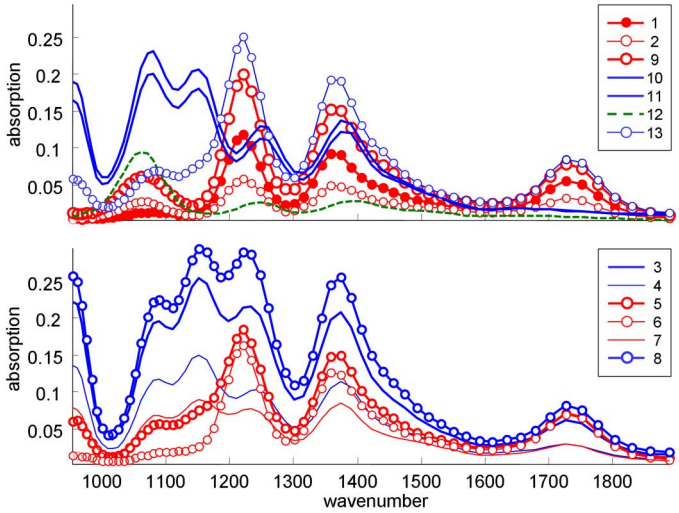

Fig. 4. IR absorption spectra of 13 mixtures with dissimilar proportions of acetone, alcohol, witch hazel, and water obtained by the instrument. For visualization purposes, mixtures are separated into those that contain witch hazel (top) and those that do not (bottom). Blue lines denote high concentration of IPA; circles denote high concentration of acetone.

A. Experimental Procedure

Mixtures were prepared in the liquid phase. No treatment of the analyte or mixture prior to sampling was performed. Each analyte was inserted into a glass vial, whose headspace was directly placed in the gas flow path. IR spectra were recorded from the headspace of the liquid mixtures, pressurized to 12 psig in the gas cell. Lock-in chemical excitation with a carrier frequency of 0.05 Hz was used as a sampling technique to improve SNR. Five cycles were executed per sample, and the resulting spectra were averaged.

B. Results

Fig. 3 shows the IR absorption spectra of the individual mixture components, as detected by the instrument. These spectra can be shown to be quantitatively similar to those obtained with FTIR , [11]. In turn, Fig. 4 shows the IR absorption spectra for the 13 mixtures. Partial least squares (PLS) regression [12] was used to build a calibration model for the concentration of acetone. A two-loop leave-one-out (LOO) cross-validation procedure was used to select a suitable number of latent variables

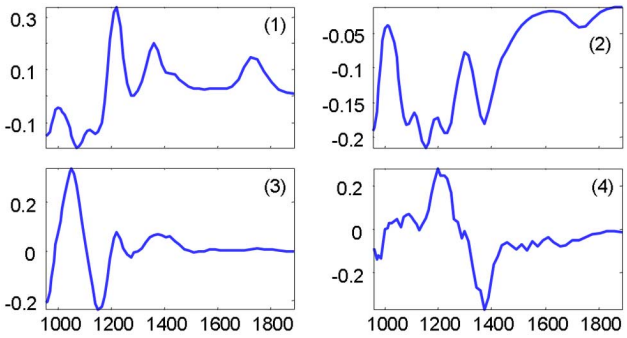

Fig. 5. First four latent vectors of the PLS model. Note how the first latent variable closely resembles the IR spectra for acetone.

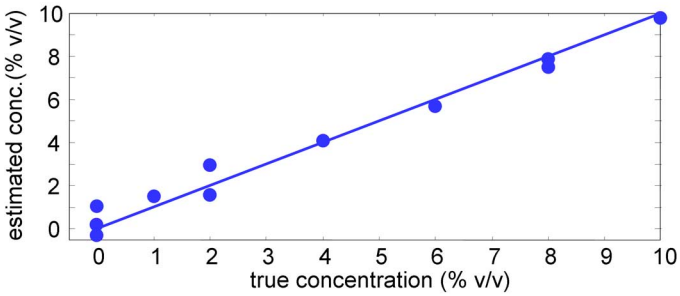

Fig. 6. Estimated concentration of acetone using PLS regression calibration and LOO cross-validation.

(inner loop) and train the regression coefficients (outer loop). The number of latent vectors that minimizes the mean-square-error (MSE) of the acetone concentration estimate was found to be equal to four, which is the same as the number of mixture components. This is attributed to the fact that IR absorption responds linearly to changes in concentration. Thus, the total number of degrees of freedom (i.e., sources of variability) equals the number of mixture components, provided that the mixture components have distinct spectra.

Shown in Fig. 5, the PLS latent vectors (loadings) can be interpreted in terms of the LVF spectra in Fig. 3, i.e., the location and shape of the prominent peaks in the first latent vector closely resembles those in the absorption spectrum of acetone. The calculated MSE error estimate for PLS was 0.47, whereas the correlation coefficient between true and estimated concentrations was equal to 0.98, as shown in Fig. 6.

V. Experimental: Analysis of Edible Oils and Fats

We also evaluated the instrument on two scenarios that resemble realistic applications: adulteration of oils and TFA detection. These applications are possible because oils and fats have well-defined IR absorption peaks in the LVF region. We first provide a general background on the chemical properties and IR absorption of oils and fats, and motivate the need for these two applications.

A. Analysis of Edible Oils and Fats

Edible oils and fats are composed primarily of saturated and unsaturated fatty acids. A fatty acid is a carboxylic (i.e., organic) acid with a typically long aliphatic (i.e., open-chain) structure. A fatty acid is said to be saturated if it contains no double bonds between carbon atoms in the aliphatic chain, thus becoming fully *saturated* with hydrogen atoms. On the contrary, unsaturated fatty acids contain carbon chains with double bonds. If an unsaturated fatty acid contains only one double bond in the aliphatic structure, it is referred to as monounsaturated. Likewise, if it contains more than one double bond between the carbon atoms, it is referred to as polyunsaturated. Unsaturated fatty acids in naturally occurring edible oils are found in the *cis* ("on the same side," in Latin) configuration. The presence of double bonds in unsaturated oils makes them more chemically reactive than saturated fats. In fact, the reactivity is proportional to the number of double bonds in the carbon chain. Therefore, unsaturated fatty acids, particularly polyunsaturated are extremely vulnerable to heat, oxygen, and light, which makes them unsuitable for the use in nonperishable food products [13].

In order to make oils and fats more resistive to oxidation and rancidity, manufacturers typically employ an industrial process called hydrogenation, which consists of adding hydrogen atoms to unsaturated double bond sites. Specifically, in this process, hydrogen atoms are added to oils at elevated temperatures in the presence of a metal catalyst. The hydrogenation process results in either partially or fully hydrogenated fatty acids. Partial and full hydrogenation differ mainly in the number of unsaturated fatty acids in the *trans* ("on the opposite side," in Latin) configuration left as a byproduct of the hydrogenation process, and in the degree of saturation achieved. Full hydrogenation yields a higher percentage of saturated fats per volume than partial hydrogenation with almost no trans-fatty acids. Furthermore, hydrogenation raises the melting point of oils, and the resulting substance is typically in a semisolid or solid state at room temperature, such as margarine and shortening. Most of the commercially available margarines, spreads, and shortenings are manufactured through the partial hydrogenation of soybean oil, and contain a considerable amount of TFAs. The consumption of TFAs increases the risk of coronary heart disease, and has been in the center stage of debate by health activists [14].

The mid-IR region contains a wealth of information about the characteristic molecular vibration frequencies of edible oils and fats. Table II lists the frequency bands and shoulders of edible oils in the mid-IR region, along with the assigned functional group, mode of vibration and intensity [15]. Fig. 7 illustrates the IR absorption spectrum of olive oil in the mid-IR region, obtained by an FTIR instrument, as well as the spectra obtained by our LVF instrument. The numbers atop each major peak indicate the frequency band assignment according to Table II. Six vibration frequencies seem to strongly contribute to the IR absorption spectrum obtained by both instruments. Although at a lower resolution, our instrument is able to capture the influence of all the major absorption peaks, and a clear correlation can observed with the high resolution spectra from the FTIR instrument.

B. Oil Adulteration

Among the many applications of oil discrimination using IR spectroscopy, the determination of authenticity for the prevention of food fraud is an important one. Food fraud consists of

TABLE II
TWENTY- FIVE IMPORTANT FREQUENCY BANDS AND SHOULDERS OF EDIBLE OILS IN THE MID-INFRARED REGION, ALONG WITH THE ASSIGNED FUNCTIONAL GROUP, MODE OF VIBRATION AND THE INTENSITY. ADAPTED FROM [15]

No.	*Frequency* (cm^{-1}) [a]	*Functional Group*	*Mode of vibration*	*Intensity* [b]
1	3468 (b)	–C=O (ester)	Overtone	w
2	3025 (s)	=C–H (*trans*-)	Stretching	vw
3	3006 (b)	=C–H (*cis*-)	Stretching	m
4	2953 (s)	–C–H (CH_3)	Stretching (asym)	m
5	2924 (b)	–C–H (CH_2)	Stretching (asym)	vst
6	2853 (s)	–C–H (CH_2)	Stretching (sym)	vst
7	2730 (b)	–C=O (ester)	Fermi resonance	vw
8	2677 (b)	–C=O (ester)	Fermi resonance	vw
9	1746 (b)	–C=O (ester)	Stretching	vst
10	1711 (s)	–C=O (acid)	Stretching	vw
11	1654 (b)	–C=C– (*cis*-)	Stretching	vw
12	1648 (b)	–C=C– (*cis*-)	Stretching	vw
13	1465 (b)	–C–H (CH_2,CH_3)	Bending (scissoring)	m
14	1418 (b)	=C–H– (*cis*-)	Bending (rocking)	w
15	1400 (b)		Bending	w
16	1377 (b)	–C–H (CH_3)	Bending (sym)	m
17	1319 (b,s)		Bending	vw
18	1238 (b)	–C–O, –CH_2 –	Stretching, bending	m
19	1163 (b)	–C–O, –CH_2 –	Stretching, bending	st
20	1118 (b)	–C–O	Stretching	m
21	1097 (b)	–C–O	Stretching	m
22	1033 (s)	–C–O	Stretching	vw
23	968 (b)	–HC=CH– (*trans*-)	Bending out of plane	w
24	914 (b)	–HC=CH– (*cis*-)	Bending out of plane	vw
25	723 (b)	–$(CH_2)_n$–, –HC=CH– (*cis*)	Bending (rocking)	m

[a] b, band; s, shoulder.
[b] w, weak; vw, very weak; m, medium; vst, very strong; st, strong.

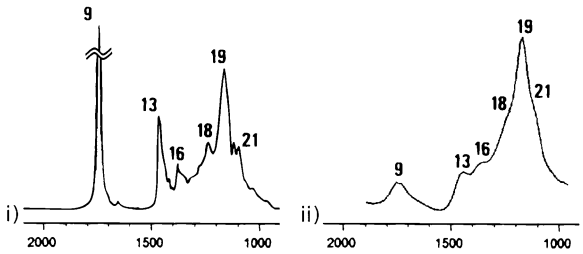

Fig. 7. IR absorption spectrum of olive oil in the mid-IR region. i) Spectrum obtained by a high-resolution FTIR spectroscope [15]. ii) Spectrum obtained by our LVF instrument. The numbers atop each major peak indicates the frequency band assignment in Table II.

the adulteration of food products by substituting something of higher value with something of lower grade, typically for the purpose of economic gain. Food fraud is viewed as a serious issue by the United States Food and Drug Administration (FDA), since it can make it "difficult for honest companies to compete in the marketplace" [16] and, more importantly, can cause severe health problems for consumers. Because of its superior flavor and potential health benefits, olive oil is typically sold at a premium when compared to other vegetable oils. Many approaches for the detection of olive oil adulterations using IR absorption spectroscopy have been previously reported [17], [18]. The purpose of this study is to demonstrate our instrument's capabilities for the classification of oils.

1) Experimental Procedure: Five samples of commercial products were obtained from local supermarkets. The collection includes all major oils used in the North American diet. Table III

TABLE III
COMPOSITION OF THE SAMPLES AS PROVIDED BY THE PRODUCERS

Fat	*Canola*	*Peanut*	*Corn*	*Safflower*	*Olive*
Saturated (%)	7.1	17.9	14.3	7.1	14.3
Trans (%)	0.0	0.0	0.0	0.0	0.0
Polyunsat (%)	28.6	35.7	57.1	71.4	10.7
Monosat (%)	57.1	42.3	28.6	14.3	71.4

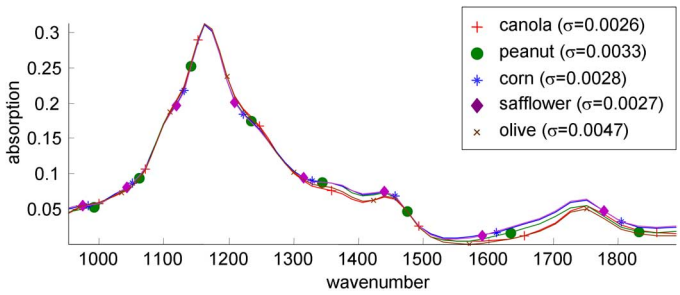

Fig. 8. IR absorption spectra of five edible oils obtained by the instrument. Within-class standard deviation shown in parenthesis.

shows the composition of each sample. A 0.0125 mm Teflon spacer was placed between two ZnSe disks, and the gap was filled with a thin (i.e., 6 μL) oil film. Five spectra were collected from each sample. Each spectrum was obtained by placing the liquid cell in the light path, and immediately recording and averaging 250 continuous measurements at 1 Hz. Since the IR beams are collimated, and because of relatively low SNR, we neglect artifacts that may arise due to scattering of light, and use the B-L Law in its original form to calculate absorption.

2) Results and Discussion: The average response and standard deviation of the acquired IR absorption spectra for each class are shown in Fig. 8. It can be observed that the oil spectra are nearly identical, which makes the classification problem nontrivial. However, there are a few subtle but systematic differences in these spectra that can be amplified via preprocessing techniques. Since absolute concentration is irrelevant to the classification of samples, we perform vector normalization on each spectrum, and use the normalized spectra for all further manipulations. It has been reported that the classification rate of similar oils improves when using the second derivative spectra [19]. Thus, we take the second derivative of the spectra, and perform plus-L-minus-R (PLMR) feature selection [20] to retrieve a subset of features for classification. The PLMR criterion for selecting or removing features is based on classification rate obtained via a nearest-neighbor rule [20] using Euclidean distance as a proximity measure and LOO cross-validation. The parameters for the PLMR algorithm are $\mathrm{L} = 4$ and $\mathrm{R} = 3$, and the algorithm is stopped when the classification rate decreases or ceases to improve. The algorithm returns two features (wavenumbers 968 and 1109 cm^{-1}) of the second derivative spectra; Fig 9 shows a scatterplot of these two features for all samples, which indicates that the system provides linear separability for the five oils. Interestingly, the ratio between these two features has been shown to be correlated with the level of poly-unsaturation in edible oils [21]. Further, classification of oil spectra using these two features and a nearest-neighbor rule yields 100% correct classification on unseen data (i.e., through LOO).

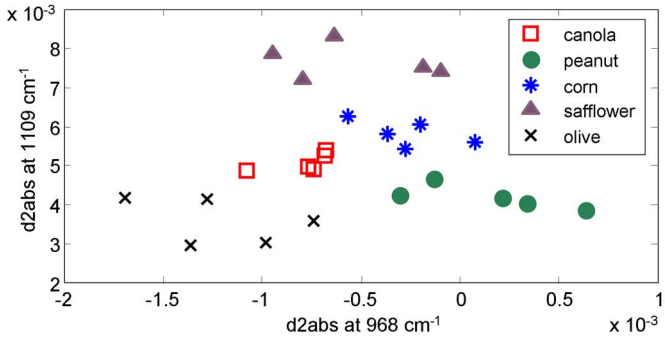

Fig. 9. Second derivative spectra at 968 versus 1109 cm^{-1} for all oil samples.

TABLE IV
COMPOSITION OF THE SAMPLES AS PROVIDED BY THE PRODUCERS

Class	*1*	*2*	*3*	*4*	*5*	*6*
Producer	Country Crock	Country Crock	Country Crock	Country Crock	Imperial	Imperial
Type	Margarine	Margarine	Spread	Spread	Spread	Spread
Packaging	Tub	Stick	Tub	Stick	Tub	Stick
Serving(g) [a]	14.0	14.0	14.0	14.0	14.0	14.0
Total Fat(g) [a]	11.0	11.0	7.0	8.0	7.0	9.0
Saturated(%) [b]	18.2	18.2	21.4	18.7	21.4	22.2
Trans(%) [b]	9.1	27.2	7.1	25.0	7.1	27.8
Polyunsat(%) [b]	45.4	22.7	50.0	31.2	42.9	22.2
Monosat(%) [b]	27.3	31.9	28.6	31.2	21.4	27.8

[a] approximate values given by manufacturers; rounded to the nearest decimal.
[b] percentage of total fat.

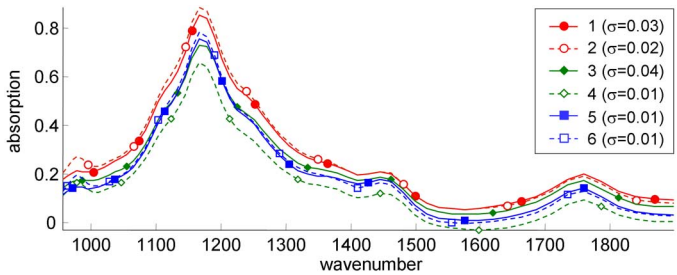

Fig. 10. IR spectra of margarine and spread samples. Dashed and solid lines represent samples in stick and tub packages, respectively. Three replicates per sample are shown (within-class standard deviation in parenthesis).

C. Trans-Fatty Acid (TFA) Detection

Recently, there has been a growing concern about the increased risk of coronary heart disease (CHD) due to the consumption of TFAs [22]. Specifically, TFA has been shown to raise low-density lipoprotein cholesterol (LDL-C or "bad" cholesterol), which is a major risk factor of CHD. Based on metabolic studies conducted in 1997 [22], it is estimated that approximately 30 000 premature deaths per year in the United States can be attributed to consumption of TFA. TFA health threats have prompted the FDA to require mandatory labeling of TFA content in manufactured food products. The FDA allows manufacturers to choose which methodology to use for obtaining the trans fat content in foods, but indicates that the official methods from the Association of Official Analytical Chemists (AOAC) and the American Oil Chemists Society (AOCS) are considered appropriate and compliant with trans fat nutrition labeling requirements [13]. The AOAC and AOCS organizations' official methods are based on IR absorption spectroscopy or gas chromatography. Among the main advantages of IR absorption spectroscopy over gas chromatography are the reduced sample preparation time and the ability to perform online measurements through the attenuated total reflection (ATR) method [13]. Online measurements are particularly important for real-time monitoring of heat-induced trans fat formation in food products. However, for offline measurements, transmission methods can also produce reliable results. In order to comply with FDA labeling requirements, TFA content below 0.5 g may be reported as 0 g. Likewise, TFA content must be labeled at increments of 0.5 g, and is considered to be misbranded if the nutrient content of the composite samples exceed 120% of labeling value [23].

1) Experimental Procedures: To determine the extent to which our instrument could be used for the detection of TFA in food products, we performed experiments with commercially available margarine and spreads sold in two different packages: sticks and tubs. Six samples of commercial products were obtained from local supermarkets. The collection includes three pairs of spread and margarine from two major brands. Table IV shows the class assignment and composition of each sample. Since margarine and spreads are water-in-oil emulsions, the samples were melted to obtain samples consisting of only oil [13]. IR spectra were recorded following the same experimental procedure used with the edible oils. Three spectra were collected from each sample.

2) Results and Discussion: Fig. 10 shows the IR absorption spectra of margarine and spread samples. The solid and dashed lines in the figure represent samples in stick form and tub packages, respectively. By carefully examining Fig. 10, we can observe a systematic difference on the fingerprint region between the spectra of samples from the two types of packaging. The distinction is more evident near 968 cm^{-1}, which is precisely where the TFA IR absorption band is centered (see Table II). The type of packaging used indicates the consistency of the margarine or spread. Tub margarines are softer because they have a higher ratio of liquid oil to hydrogenated fat when compared with stick form. Since the process of partial hydrogenation yields unsaturated fatty acids in the transconfiguration (which are in semisolid or solid state at room temperature), typically the more solid the margarine or spread is, the higher the TFA content present.

Since the main ingredient of the selected margarines and spreads is soybean oil, we used the difference spectra to remove the contribution of soybean oil from the mixture with a least-squares procedure. The result of this difference spectra method at the TFA absorption band is illustrated in Fig. 11. Following Thomsen *et al.* [24], we estimate the TFA limit of detection (LOD) as follows:

$$S = (27.8\% - 7.1\%)/(0.0421\,\text{abs} - 0.0085\,\text{abs}) = 616\%/\text{abs}$$

where abs represents dimensionless absorbance units, as in (1), S is the ratio of TFA, as shown in from Table IV, per absorption for classes 5 and 6. The absorption values 0.0421 and 0.0085 are

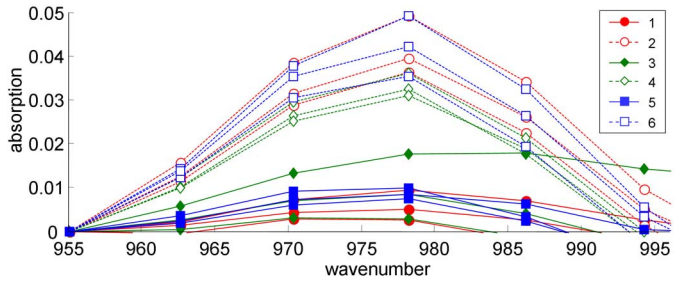

Fig. 11. TFA IR absorption band of margarine and spreads after the subtraction of the IR spectrum of soybean oil.

computed as the average absorptions at 978 cm^{-1} for classes 5 and 6, respectively (from Fig. 11).

Using $s_{bi} = 0.0053$ (average sample standard deviation of all classes), we obtain a TFA detection limit expressed as relative concentration c_L with respect to total fat of [24]:

$$\text{c}_\text{L} = 3 \times s_{bi} \times S = 3 \times 0.053 \times 616 = 9.8.\%$$

Thus, we estimate LOD for the class with highest fat content per serving (a worst case scenario approximation) in terms of weight as follows:

$$\text{LOD} = 9.8\% \times 11\text{g} \approx 1\text{g}.$$

Though the estimated LOD of 1 g is above the necessary LOD for compliance with FDA labeling requirements, automation of the liquid sampling procedure (which was done manually in our experiments) could dramatically improve the worst case LOD reported here. Moreover, our results shown that the instrument can be used for the classification of margarine and spreads according to TFA levels; based on the available samples, a nearest-neighbor classifier with LOO cross-validation is able to successfully classify all samples into either high-TFA or low-TFA content. These results indicate that the detection of high levels of TFA content in food products is possible using the instrument.

VI. Conclusion and Future Work

IR absorption spectroscopy is a powerful analytical technique for the qualitative and quantitative analysis of chemicals. The widespread use of this technique beyond the laboratory has been hampered by the cost, robustness, and portability of the instruments. In this research, we have integrated a low-cost IR absorption spectroscope based on LVF technology for the automated detection of gases and vapors, and the semi-automated detection of liquids.

Despite operating at low-resolution, LVF-based spectroscopy is a promising method for the characterization of chemicals. We have demonstrated the use of the instrument for two real-world applications in the edible oils and fats domain: oil adulteration and TFA detection. We have shown that the spectra of peanut, corn, canola, safflower, and olive oil obtained by the instrument can be fully classified via statistical pattern recognition techniques, and that we can successfully distinguish products (e.g., spreads and margarine) by their levels of TFA content. Furthermore, when combined with chemometrics techniques, the instrument can be used to determine the concentration of an analyte (i.e., acetone) in a matrix of other simple and complex absorbing species (i.e., water, alcohol, and witch hazel, in our case) with a high level of precision (i.e., uncertainty of $\pm 0.8\%$). Clearly, this uncertainty estimate depends largely on the characteristic IR spectra of the samples and matrices, and therefore should not be generalized to other calibration problems. Nonetheless, these results suggest that LVF-based spectroscopy is a viable analytical technique for the characterization of liquids and concentrated gases in niche applications.

Several directions for improvements are being considered at the time of this writing, the most critical being enhancing the detection limit for gas measurements. This could be accomplished in several ways. First, a preconcentrator could be used to enrich the sample by a factor of 10–100 before it is delivered to the gas cell. Thus, since absorption is linearly dependent on concentration, detection limit could be improved by a similar factor. Second, a long-path gas cell could be used to improve the detection limit of the system, since absorption is linearly dependent on the distance traveled by the IR radiation through the sample. For instance, microstructured fibers offering guidance through an air core, such as photonic bandgap or random-hole optical fibers), could provide longer interaction lengths, thus greatly enhancing the detection of trace chemicals in gases or liquids at the expense of longer (i.e., two orders of magnitude) sampling times [25], [26]. Furthermore, instrument purging and pressurization with a nonabsorbing gas in the LVF region could be used to avoid saturation and improve detection for trace gases in the long-path gas cell. Third, a pyrolyzer could be used to improve sample discrimination. Pyrolysis decomposes organic materials by controlled heating in the absence of oxygen, rendering the sample into a more suitable form for a subsequent analytical procedure. For the purpose of trace gas detection, pyrolysis could increase the concentration of the sample's volatile and semi-volatile compounds. Likewise, by fractionated pyrolysis, fractions of the sample could be analyzed at different temperatures and different times, thus further improving sample discrimination. Fourth, a circulation pump could be used to bring the concentration of the measurand gas to the headspace saturation levels. By adding a temperature controller at the sample cell, we could further improve SNR, particularly for liquid measurements, since IR spectral responses are greatly affected by the temperature of the analyte, as well as that of the windows. Finally, improvements in spectral resolution could be obtained by using a larger array of pyroelectric sensors (e.g., 128 or 256 pixels) coupled with higher resolution LVFs [27], with the tradeoff of increased cost.

References

[1] K. Persaud and G. Dodd, "Analysis of discrimination mechanisms in the mammalian olfactory system using a model nose," *Nature*, vol. 299, pp. 352–355, 1982.

[2] C. Pinheiro, C. M. Rodigues, T. Schafer, and J. G. Crespo, "Monitoring the aroma production during wine-must fermentation with an electronic nose," *Biotechnol. Bioeng.*, vol. 77, pp. 632–640, 2001.

[3] T. Nagle, S. S. Schiffman, and R. Gutierrez-Osuna, "The how and why of electronic noses," *IEEE Spectrum*, vol. 35, pp. 22–34, 1998.

[4] C. P. Bacon, Y. Mattley, and R. DeFrece, "Miniature spectroscopic instrumentation: Applications to biology and chemistry," *Review of Scientific Instruments*, vol. 75, pp. 1–16, Jan. 2004.
[5] E. R. Badman and R. G. Cooks, "Miniature mass analyzers," *J. Mass Spectrum*, vol. 35, pp. 659–671, 2000.
[6] R. Rubio, N. Sabate, C. Calaza, J. Santander, L. Fonseca, I. Gracia, C. Cane, M. Moreno, and S. Marco, "Optical simulation of a MOEMS based tuneable Fabry-Perot interferometer," in *Proc. IEEE Sensors*, 2004, vol. 3, pp. 1324–1327.
[7] R. Rubio, J. Santander, J. Fonollosa, L. Fonseca, I. Gracia, C. Cane, M. Moreno, and S. Marco, "Exploration of the metrological performance of a gas detector based on an array of unspecific infrared filters," *Sens. Actuators B: Chemical,*, vol. 116, no. 1–2, pp. 183–191, Jul. 28, 2006.
[8] B. Stuart, *Infrared Spectroscopy: Fundamentals and Applications*. Kent, U.K.: Wiley, 2004.
[9] W. Schmidt, *Optical Spectroscopy in Chemistry and Life Sciences*. Weinheim, Germany: Wiley-VCM Verlag GmbH & Co, 2005.
[10] "The use of a lock-in amplifier for the detection and measurements of light signals," EG&G Princeton Applied Research, Wellesley, MA, T-151A-5M/10/84-EG&G, 1984.
[11] P. J. Linstrom and W. J. Mallard, "NIST Standard Reference Database Number 69," National Institute of Standards and Technology, 2003 [Online]. Available: http://webbook.nist.gov, NIST Chemistry WebBook
[12] D. M. Haaland and E. V. Thomas, "Partial least-squares methods for spectral analyses. 1. Relation to other quantitative calibration methods and the extraction of qualitative information," *Anal. Chem.*, vol. 60, pp. 1193–1202, 1988.
[13] V. Milosevic and A. Kocak, "Analyzing trans fats in edible oils and fats using single-reflection ATR-FTIR," *Amer. Lab.*, pp. 30–34, Jun. 2004.
[14] D. Mozaffarian, M. B. Katan, A. Ascherio, M. J. Stampfer, and W. C. Willett, "Trans. fatty acids and cardiovascular disease," *N. Engl. J. Med.*, vol. 354, pp. 1601–1613, Apr. 13, 2006.
[15] M. D. Guillen and N. Cabo, "Characterization of edible oils and lard by Fourier transform infrared spectroscopy. Relationships between composition and frequency of concrete bands of the fingerprint region," *J. Amer. Oil Chem. Soc.*, vol. 74, pp. 1281–1286, 1997.
[16] P. Kurtzweil, "Fake food fight," *FDA Consumer*, Mar. 1999.
[17] F. Ulberth and M. Buchgraber, "Authenticity of fats and oils," *Lipid Sci. Technol*, vol. 102, pp. 687–694, 2000.
[18] Y. W. Lai, E. K. Kemsley, and R. H. Wilson, "Quantitative analysis of potential adulterants of extra virgin olive oil using infrared spectroscopy," *Food Chem.*, vol. 53, pp. 95–98, 1995.
[19] N. Dupuy, L. Duponchel, J. P. Huvenne, B. Sombret, and P. Legrand, "Classification of edible fats and oils by principal component analysis of fourier transform infrared spectra," *Food Chem.*, vol. 57, pp. 245–251, 1996.
[20] K. Fukunaga, *Statistical Pattern Recognition*, 2nd ed. New York: Academic, 1990.
[21] M. D. Guillen and N. Cabo, "Relationships between the composition of edible oils and lard and the ratio of the absorbance of specific bands of their fourier transform infrared spectra. Role of some bands of the fingerprint region," *J. Agric. Food Chem.*, vol. 46, pp. 1788–1793, 1998.
[22] A. Ascherio, "Health effects of trans fatty acids," *Amer. J. Clin. Nutr.*, vol. 66, pp. 1006S–10S, 1997.
[23] Food and Drug Administration, " Food labeling; Trans fatty acids in nutrition labeling; Consumer research to consider nutrient content and health claims and possible footnote or disclosure statements; Final rule and proposed rule," *Federal Register 21 CFR Part 101*, vol. 68, pp. 41433–41506, 2003.
[24] V. Thomsen, D. Schatzlein, and D. Mercuro, "Limits of detection in spectroscopy," *Spectroscopy*, vol. 18, pp. 112–114, 2003.
[25] G. Pickrell, W. Peng, and A. Wang, "Random-hole optical fiber evanescent-wave gas sensing," *Opt. Lett.*, vol. 29, pp. 1476–1478, Jul. 1, 2004.
[26] M. N. Petrovich, A. Brakel, F. Poletti, K. Mukasa, E. Austin, V. Finazzi, P. Petropoulos, E. Driscoll, M. Watson, T. DelMonte, T. M. Monro, J. P. Dakin, and D. J. RIchardson, "Microstructured fibres for sensing applications," in *Proc. SPIE Optics East*, Boston, MA, Oct. 2005, pp. 23–26.
[27] R. Passerini, M. Kohli, P. Ryser, A. Seifert, B. Willing, and P.-Y. Cattin, "Room temperature spectrometry in the MIR range," in *Proc. Detectors and Associated Signal Processing*, St. Etiene, France, 2003, pp. 89–96.

Felipe G. Nogueira received the B.S. degree and the M.S. degree in computer science from Texas A&M University (TAMU), College Station, in 2002 and 2006, respectively.

In 2003, he joined Resource Studios, Inc., Houston, TX, to lead the development of their next-generation Computer Aided Facility Management solution. He is currently a Software Engineer with the Data Acquisition and Control Systems group at Schlumberger. His research interests include signal processing, machine learning, intelligent systems, and computer-human interaction.

Daniel Felps received the B.S. degree in computer engineering (Hon.) from Texas A&M University (TAMU), College Station, in 2005. He is currently working towards the Ph.D. degree at TAMU, and has been a Research Assistant in the Pattern Recognition and Intelligent Sensor Machines Laboratory since 2006.

His research interests include speech processing, pattern recognition, machine learning, and intelligent systems.

Ricardo Gutierrez-Osuna (M'00) received the B.S. degree in electrical engineering from the Polytechnic University, Madrid, Spain, in 1992, and the M.S. and Ph.D. degrees in computer engineering from North Carolina State University, Raleigh, in 1995 and 1998, respectively.

From 1998 to 2002, he served on the faculty at Wright State University. He is currently an Associate Professor of Computer Engineering at Texas A&M University (TAMU). His research interests include pattern recognition, neuromorphic computation, chemical sensor arrays, and audio-visual speech processing.

Dr. Gutierrez-Osuna is a recipient of the National Science Foundation Career Award for his research on machine olfaction with chemical sensors arrays.